Journal of Advanced Engineering Research
ISSN: 2393-8447
Volume 10, Issue 2, 2023, pp.248-261

EFFECT OF PROCESS PARAMETERS ON THE PROPERTIES OF FRICTION STIR WELD JOINTS OF AA6061-T6 ALLOY

Anandhu V.A.[1,*], Abey Vishnu Narayana[1], Jose M.J.[2]

[1]Department of Mechanical Engineering, Sree Narayana Institute of Technology Adoor, India..

[2]Department of Mechanical Engineering, Government College of Engineering Kannur, India.

[1,*] anandhuva57@gmail.com ,Tel: 7909238032

ABSTRACT

Wrought heat treatable aluminum magnesium silicon alloys per AA 6061-T6 are of medium strength and have excellent weldability compared to high strength aluminum alloys. This class of alloys is therefore widely used in ship frames, storage tanks and aircraft applications. It is not possible to use all kinds of aluminum manufacturing processes. Because most aluminum alloys are hardened, fusion welding cannot be applied because the high heat generated during the process will cause them to lose some of their properties, making them unable to perform their intended function. In 1991, the Welding Institute (TWI) invented a new technology in the welding process and named it Friction Stir Welding (FSW). FSW is a solid-state welding process in which parts are joined together at a solidifying temperature. The strength of the weld is affected by the grain size and the tensile strength of the core region of the weld. Therefore, an attempt was made to develop an artificial neural network and predict a data set related to the FSW engine and process parameters. Experimental relationships to predict grain size and tensile strength of frictional AA 6061-T6 aluminum alloy welds. The empirical relationships are developed by a fully factorial design. A linear regression relationship was also established between grain size and weld core tensile strength of FSW joints.

Keywords- Aluminum 6061-T6 S Alloy, Artificial Neural Network, Friction Stir Welding (FSW), Tensile strength of FSW joints, Welding Parameters.

1. INTRODUCTION

Metal joining is a method of joining two or more materials by external means. There is a huge demand for metal joining due to limitations of producing a large part design or complicated by conventional manufacturing processes such as casting, forging, rolling and extrusion, etc. Welding is a manufacturing technique that joins materials, usually metals or thermoplastics, causing adhesion. Welding is one of the essential and widely used manufacturing processes in any manufacturing/manufacturing industry. The main goal of welding technology is to achieve optimal conditions for perfect joints. There are mainly two types of welding; one is fusion welding and the other is solid state welding. In fusion welding, a heat source is used to melt the material and after melting pressure is applied to join the materials but solid-state welding is done below the melting temperature of the components. division, such as (FSW). Friction-stirring welding (FSW) is an emerging energy-saving, attractive and environmentally friendly solid-state welding process invented in 1991 by the Welding Institute (TWI) in the UK [5]. FSW offers many advantages over conventional fusion welding techniques, such as the absence of expensive consumable fillers, good mechanical and metallurgical properties of the formed joint, and no solidification cracks., no voids, low distortion and lower power consumption [6]. Initially, this float welding technique was used for aluminum [7] but later it was used to join magnesium [8], titanium [5], copper [9] and also iron alloys [10]. A non-consumable tool cylindrical tool is rotated at a constant speed and is inserted/plunged in-between the two separate worksheets or plates to be joined and subsequently fed at a constant rate along the joint line as shown in fig1.1.

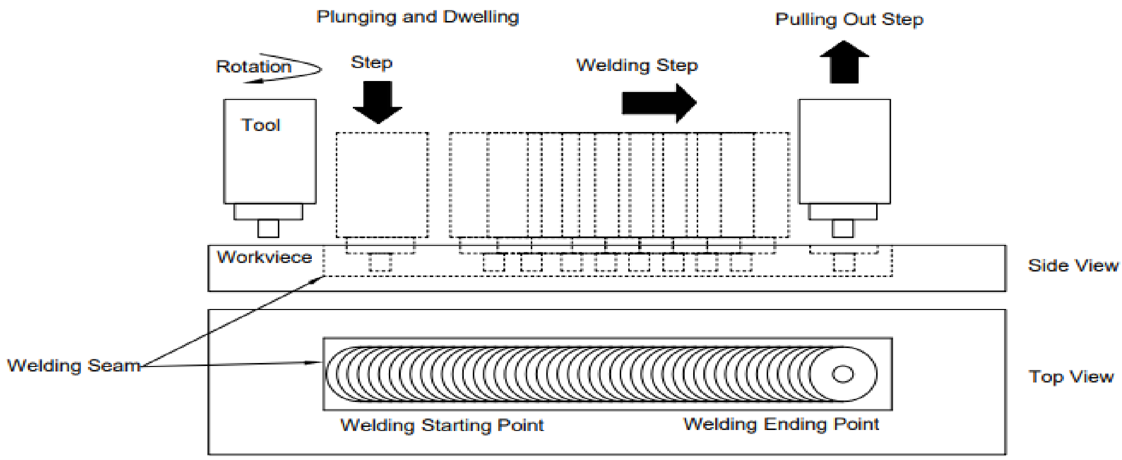

Fig.1.1. FSW process

Heat is generated within the workpiece and tool due to friction between the rotating tool shoulder and pin with the workpiece and by severe plastic deformation of the workpiece materials. Materials become soften around the pin and welding occurs while traversing along the welding direction. The main function of the non-consumable rotating tool pin is to stir the plasticized metal and move the same behind it to have a defect-free joint.

1.1. Tool Design and Its Role in Welding

Tool design is an important factor in improving both the quality of the weld or the strength of the resulting joint and the maximum welding speed that can lead to improved productivity. The design of the tool consists of two parts shoulder and peg. During FSW, most of the heat is generated by friction between the tool shoulder and the part as the shoulder strikes the part. This heat helps to soften the material and after softening, the tool pin plays a decisive role in the welding process. The main function of the non-consumable rotary tool pin is to stir the ductile metal and move it back for a good joint. The pin configuration plays an important role in the material flow. Pin tools usually have straight cylindrical stapling tool, tapered cylinder stapling tool, trapezoidal stapling tool, triangle stapling tool, straight square stapling tool, thread stapling tool, taper thread stapling tool, pentagon pin and hexagon pin tool as shown in fig.1.2.

1.2. Welding Forces

The downward force is required to maintain the position of the tool above or below the surface of the material. This force is increased when the tool is inserted into the material or mainly when the shoulder touches the part. The horizontal force acts parallel to the tool movement and is positive in the welding direction. Since this force is the result of the material's resistance to tool motion. The transverse force can be applied perpendicular to the tool's transverse direction and is defined here as positive in the forward direction of the weld. Torque is required to rotate the tool; the amount of this torque will depend on the downward force and the coefficient of friction (sliding friction) and the flow force of the material in the surrounding area (sticky friction) [6].

2. OBJECTIVES

The objective of the paper is divided into two parts. The first objective is to predict the output values corresponding to the input values by using an artificial neural network in MATLAB. The second objective of

Fig.1.2. different pin profiles

this paper is to study the effect of FSW input variables on microstructure and tensile strength of the welded joint using Minitab. Different input parameters have a significant influence on the FSW joint, they are tool rotational speed, welding speed, axial force, tool shoulder diameter, pin diameter, tool hardness. Proper controlling of these parameters helps to reduce the formation of defects in the joint. There is different software available for FSW simulation, in this work, iterative analysis is done by using the MATLAB. The mathematical model is created by MINITAB. The main objectives of this thesis are to predict the values of microstructure and tensile strength using the iterative analysis software tool (MATLAB ANN toolbox) for the selected input parameters and to investigate the effect of FSW input parameters on tensile strength and microstructure. To estimate the optimum levels of input parameters

3. METHODOLOGY

An artificial neural network created using the MATLAB toolbox. In addition, the collected data set is imported into the neuron and then trained the neuron to get a better regression and performance curve. Then simulate the sample data in the neuron and get the output of the network. These outputs are fed into the MINITAB software and analysis begins. The input and output data set of the paper "Establishment of empirical relationship to predict grain size and tensile strength of aluminium alloy 6061-T6 friction welded joint and factorial design have been collected" The full three levels are performed using the MINITAB software. A neural network model was created using MATLAB software and imported the dataset into neurons and trained the neurons to get better

the network. Simulate the neural network with sample data and collect the output of the neural network. The second step is to collect the output of the neural network as a design board response in MINITAB software. Analyse the full factorial design and perform residual plots for each parameter and perform regression models. Repeat ANOVA to obtain a statistically significant model and obtain a mathematical equation for each response parameter. Obtain key effects and interaction effects to analyse the influence of input parameters on response parameters.

3.1. Artificial Neural network's architecture

Artificial neural networks are mathematical representations of how the human brain works. The human brain is a typical model of an adaptive computer, capable of learning to respond to new inputs based on previous experience. It contains several billion neurons that are linked together to form a network. Electrical signals travel through the brain, traveling from one neuron to another through the axons that connect them in Figure 3.1.

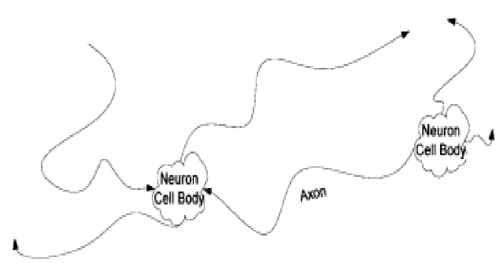

Fig.3.1. Neurons receive and transmit signals in the brain.

At each neuron, all incoming signals are combined and the amplitude is compared with the trigger threshold value. If the threshold value of a neuron is exceeded, it sends a signal to all the neurons it is connected to for further signal processing. These biological neurons are the source of the mathematical models of neural networks. The "central" element of a neural network is the neuron. Neurons are connected by a set of links, called synapses, and each synapse is described by a synaptic weight. Neurons are placed in layers, and neurons in each layer work in parallel. The first layer is the input layer. Input unit activity represents unprocessed information that has been fed into the network; In this layer, the neurons do not do any calculations. The hidden layers follow the input layer, and the activity of each hidden unit is determined from the activity of the input units and the weights at the connections of the input and hidden units. A network can have many or no hidden layers and their role is to improve the performance of the network as shown in Figure 3.2.

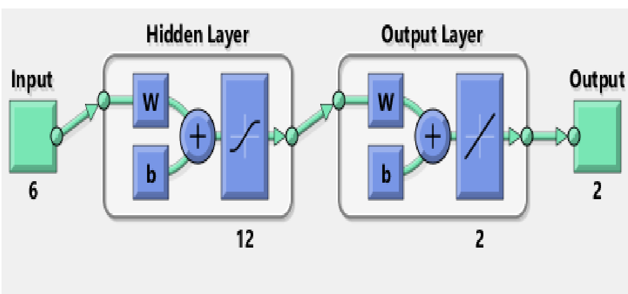

Fig.3.2. Neuron model.

The existence of these layers at the network level becomes more necessary as the number of input neurons increases. The last layer is the output layer. The behaviour of the output units depends on the operation of the hidden units and the weights between the hidden and output units. The output of the layer is the output of the entire network; neurons of the output layer, unlike the input layers, perform calculations.

There are two types of neural networks forward and recurring feeds. The feed-forwarding neural network allows the signal to travel in one direction, from input to output, i.e., the output signal of one neuron is the input of the neurons of the next layer and never vice versa. The input of the first layer is considered as the input signal of the whole network, and the output of the network is the output signal of the neurons of the last layer. In contrast, recurrent networks include feedback loops that allow signals to move forward and/or backward. The first stage of forward propagation occurs when the network is exposed to the training data and the data goes through the entire neural network to compute their predictions (labels). In other words, we route the input data through the network so that each neuron transforms the data received from the neurons of the previous layer and transmits it to the neurons of the following layer. The final layer produces label prediction results for these input samples after the data has travelled through all of the other levels and all of its neurons have finished their calculations. The loss function is then employed to calculate the loss (or error) and assess how well or poorly the projected result compares to the actual result. Once the loss has been determined, this data will be returned. This is why it is known as backpropagation. All hidden layer neurons that directly affect the output receive this loss information from the output layer. Based on the proportional contributions of each neuron to the initial output, buried layer neurons, however, only get a portion of the total missing signal. Until every neuron in the network receives a loss signal indicating their relative contribution to the total loss, this process is repeated layer by layer.

The learning algorithm starts with (often random) values for the network parameters (weights in wij and biases in bj). It takes a set of samples of the input data, passes them through the network to get predictions, compares these obtained predictions to the expected label values, and computes the loss. Perform backpropagation to propagate this loss to each parameter that makes up the neural network model, and use this propagated information to update the neural network parameters with gradient descent, reducing the overall loss. Help us get a better model. Repeat the previous steps until you feel you have a good model.

3.2. Analysis in Minitab

Originally designed as a tool for teaching statistics, Minitab is a general-purpose statistical software package designed to be interactive and easy to use. Minitab is well suited for educational use, but powerful enough to be used as a primary analysis tool for research data. The first step is to analyse the FSW process and create a factor design table to enter the factor names and levels. Finally, the design board is created. Insert response parameters and factorial design analysis. Perform factor diagram and regression analysis for each answer. Get statistically significant samples using repeated ANOVA for reliable results.

TABLE.3.1. Design table

↓	C1 StdOrder	C2 RunOrder	C3 PtType	C4 Blocks	C5 speed	C6 welding speed	C7 axial force	C8 shoulder dia	C9 pin dia	C10 hardness
1	229	1	1	1	924.0	107.560	10.370	14.995	5.095	243.0
2	250	2	1	1	1399.5	12.430	5.620	7.860	7.570	243.0
3	66	3	1	1	924.0	12.430	10.370	14.995	2.620	956.0
4	497	4	1	1	1875.0	12.430	5.620	14.995	2.620	599.5
5	228	5	1	1	924.0	107.560	10.370	14.995	2.620	956.0
6	311	6	1	1	1399.5	12.430	10.370	14.995	5.095	599.5
7	247	7	1	1	1399.5	12.430	5.620	7.860	5.095	243.0
8	717	8	1	1	1875.0	107.560	10.370	14.995	5.095	956.0
9	193	9	1	1	924.0	107.560	7.995	7.860	5.095	243.0
10	703	10	1	1	1875.0	107.560	10.370	7.860	2.620	243.0
11	670	11	1	1	1875.0	107.560	5.620	22.130	5.095	243.0
12	554	12	1	1	1875.0	12.430	10.370	14.995	5.095	599.5
13	716	13	1	1	1875.0	107.560	10.370	14.995	5.095	599.5
14	153	14	1	1	924.0	59.995	10.370	14.995	7.570	956.0
15	556	15	1	1	1875.0	12.430	10.370	14.995	7.570	243.0

4. RESULTS AND DISCUSSIONS

By using the artificial neural network to predict the output response corresponding to the input design as in the design table. The analysis is done with the output response and to find the input parameter for the optimum conditions of the output response.

4.1. Artificial Neural Network

The neuron model was created using the NN toolbox in MATLAB and to input the input and output feedback from [36]. Train the network for optimal performance, regression and training curves. Power curves show neuron performance. It consists of training, validation, and test curves, as shown in Figure 4.1. Power curves plotted in MSE versus epoch. The best validation performance is 181.9123 at epoch 43. An epoch is a measure of how many times every training vector is used once to update the weights. In batch training, all training patterns are run simultaneously in the training algorithm for one epoch before the weights are updated. The root mean squared error function is a fundamental performance function that directly affects the network. Such error reduction will lead to an efficient system. The training curve (blue curve) progresses with the Mean Squared Error (MSE) value decreasing, which means that the neuron training has minimal error with the target value. The red curve is the neuron test curve and the green curve is the validation curve, these two curves change gradually, while minimizing the MSE. So, we have better simulation results. The training curve shows the training state of the neuron at the training stage as shown in Figure 4.2. The regression line consists of four histograms: training regression, validation regression, test regression, and global regression as shown in figure 4. 3. The integer regression values are in the range of 0.99, which means the value is suitable for prediction predict the data and the error will be minimal or negligible. The sample is simulated using the neural network and exported the network output as shown in table 4.1.

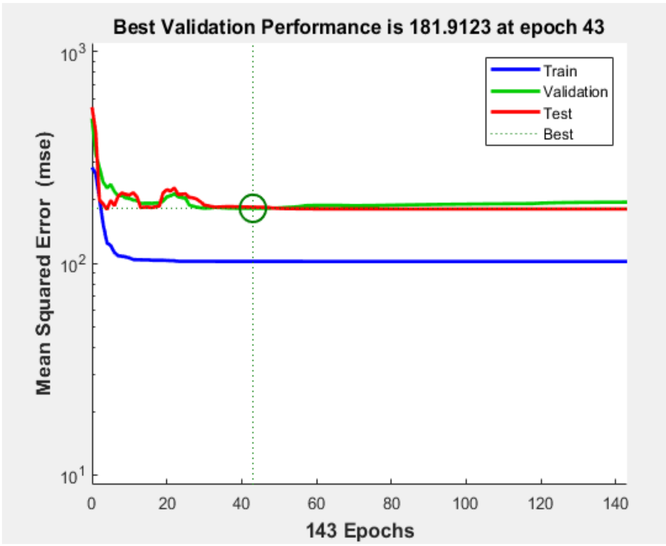

Fig.4.1. Performance curve.

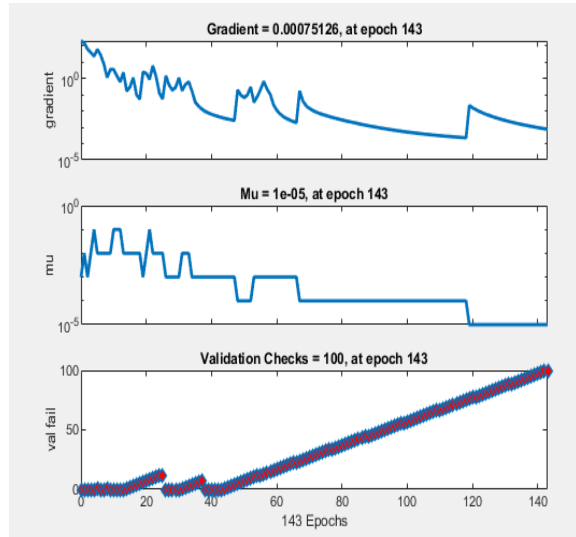

Fig.4.2. Training state.

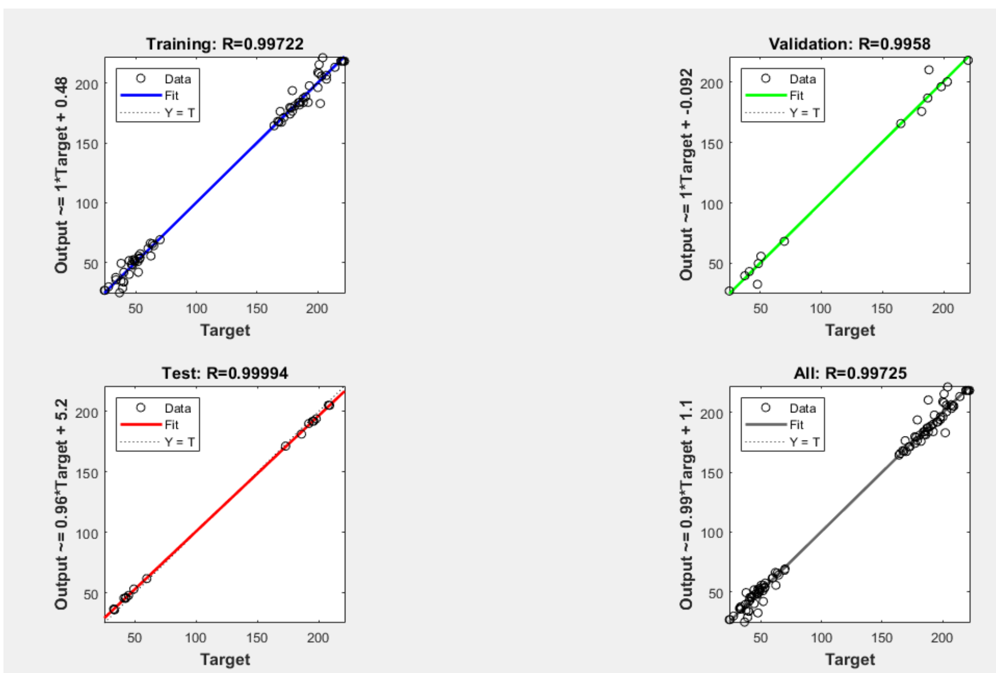

Fig.4.3. Regression graph.

TABLE.4.1. Network output

Sl.no	Weld Nugget Grain Size(Mm)	Tensile Strength (Mpa)
1	77.51006	146.6985
2	80.88226	141.5462
3	80.49316	146.8263
4	55.50958	179.4671
5	91.05074	125.3541
6	51.50391	180.3982
7	69.34828	164.8372
8	56.95988	177.9051
9	63.97783	164.6354
10	40.66451	191.6283
11	48.76775	181.9123
12	30.67212	209.9548
13	43.3155	197.064
14	61.32025	166.933
15	48.04868	190.788

4.2. MINITAB Analysis

A fully factorial design is one in which researchers measure responses to all combinations of factor levels. The number of runs required for a full 2-level factorial design is 2^k, where K is the number of factors. In our work we work with 6 elements with 3 levels, so we chose the general full factorial design.

The weld nugget size and tensile strength are response factors and tool rotation speed, welding speed, axial force, tool shoulder diameter, spindle diameter and tool stiffness are parameters. number of inputs for the design. Analysing these factors in a full factorial design yields the remaining histograms of the individual response factor. The residual plots contain graphs of normal probability, vs fit, histogram, vs order, as shown in Figures 4.4 and 4.5. A residual plot is a graph used to test fit in regression and ANOVA. By examining the remaining cells, you can determine whether the ordinary least-squares assumptions are met. If these assumptions are met, ordinary least-squares regression produces unbiased coefficient estimates with minimal variance.

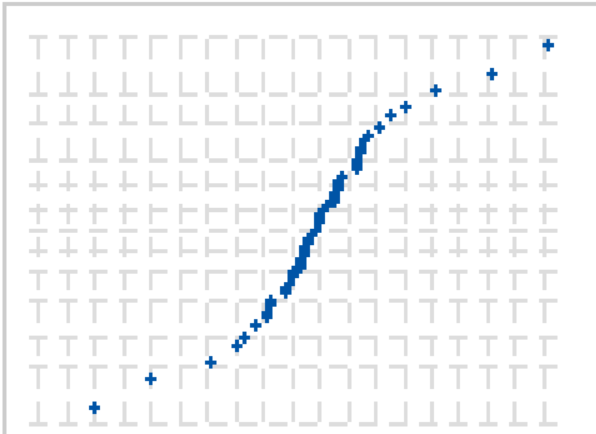

Fig.4.4. S-curve implies a distribution with long tails.

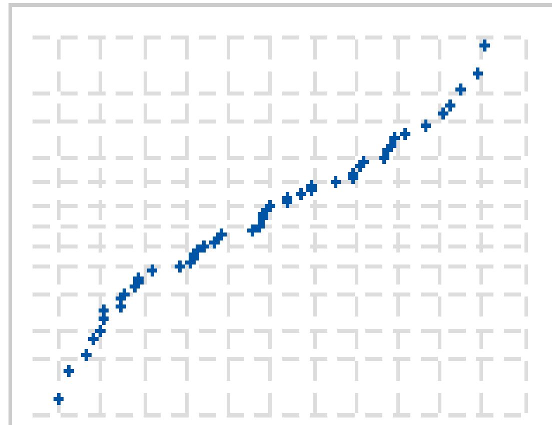

Fig.4.5. Inverted S-curve implies a distribution with short tails.

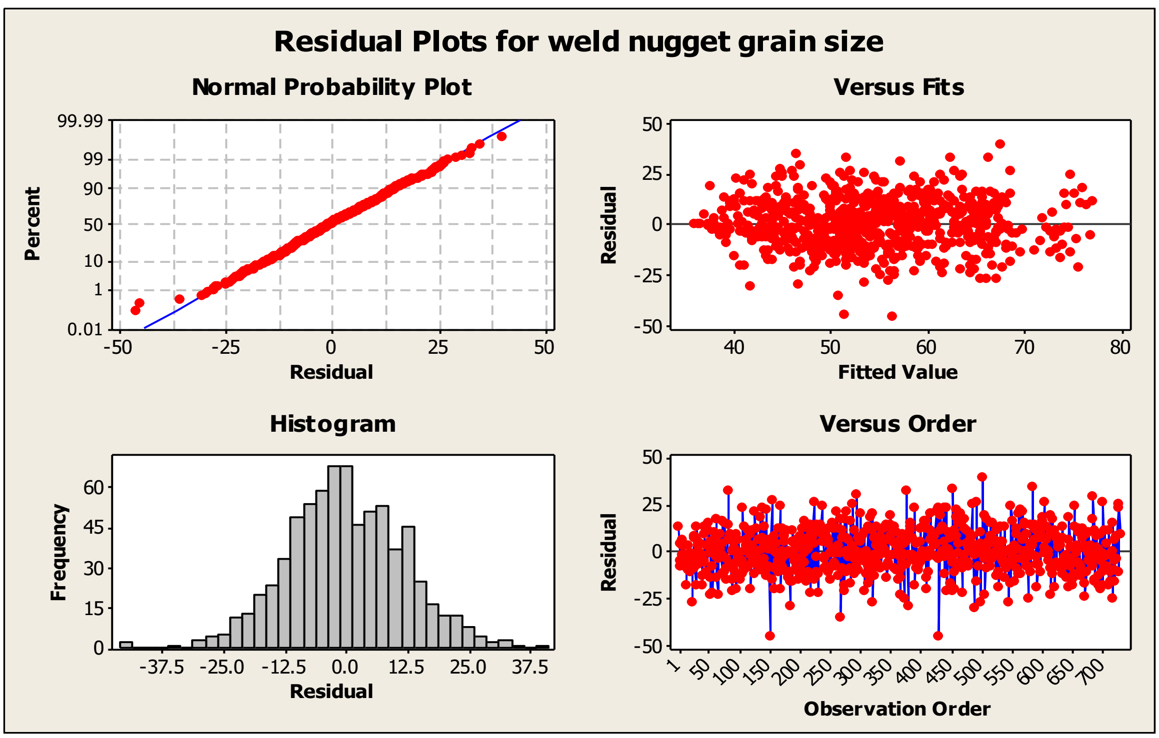

Fig.4.6. Residual plots for weld nugget grain size.

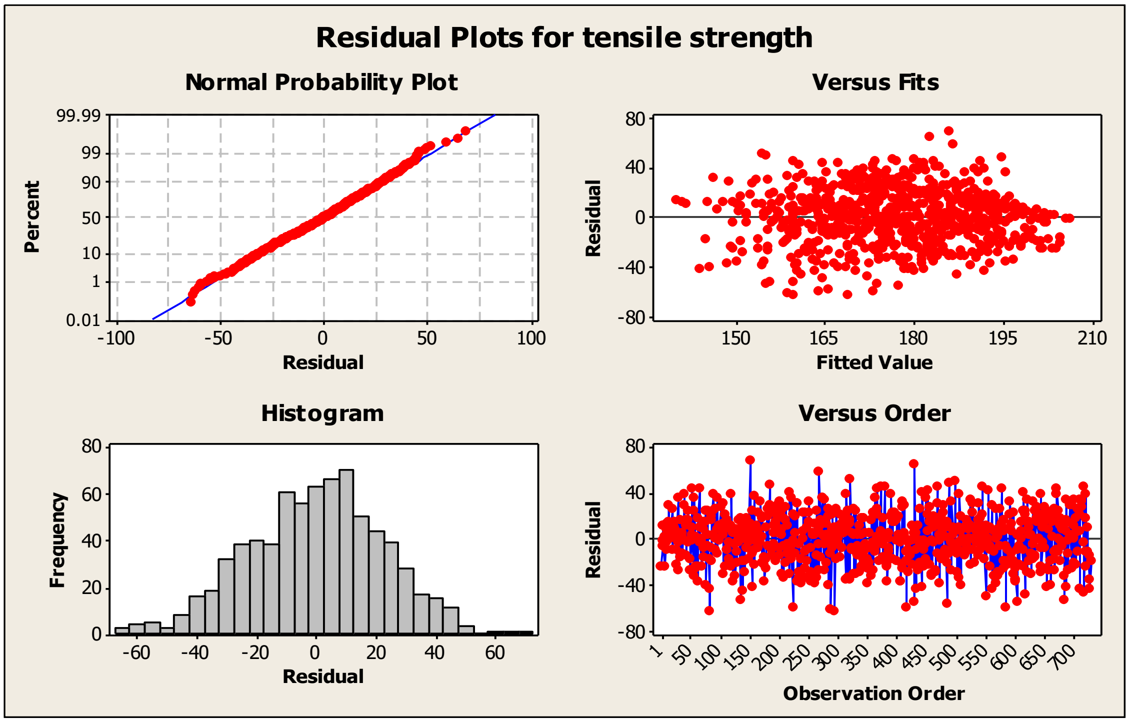

Fig.4.7. Residual plots for tensile strength.

The normal probability plot of the residuals should approximate a straight line. The samples shown in the figure violate the assumption that the residuals are normally distributed. The S-curve implies a long-tailed distribution. The inverted S-curve implies a short-tailed distribution. Use the normal probability plot of the residuals to test the assumption that the residuals are normally distributed. The normal probability histogram of the residuals should approximate a straight line.

When conducting a residual analysis, a "residuals versus fits plot" is the most frequently created plot. It is a scatter plot of residuals on the y axis and fitted values (estimated responses) on the x axis. The plot is used to detect non-linearity, unequal error variances, and outliers.

The residuals are displayed in the data collection order in a residual vs. ordinal graphic. To verify the notion that the residuals are independent, use the residuals vs. order plot. If independent residuals are analysed chronologically, no trends or patterns are apparent. The distribution of the points would suggest that correlated residuals are less likely to be independent than those that are near in space. The plot residuals ought to be randomly distributed around the central line.

A histogram is a display that indicates the frequency of specified ranges of continuous data values on a graph in the form of immediately adjacent bars. Interval An interval is a range of data in a data set. Each rectangle represents the numbers of frequencies that lie within that particular class interval. Analyse the histogram to see whether it represents normal distribution whole values of residual are fit with the residual plots of each response so that the design is good.

The main effects and interaction effects are also plotted to predict the optimum condition of the input parameters for the sound welded joint (quality responses). The main effects plot displays the means for each group within a categorical variable.

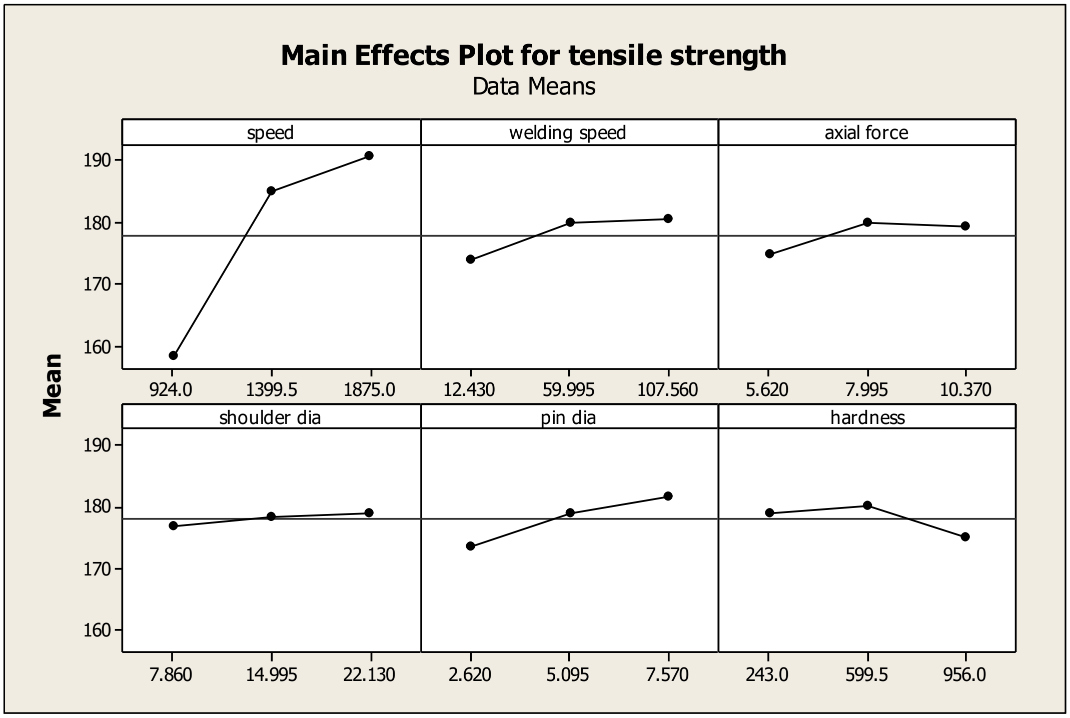

Fig.4.8. Main effect plots for tensile strength.

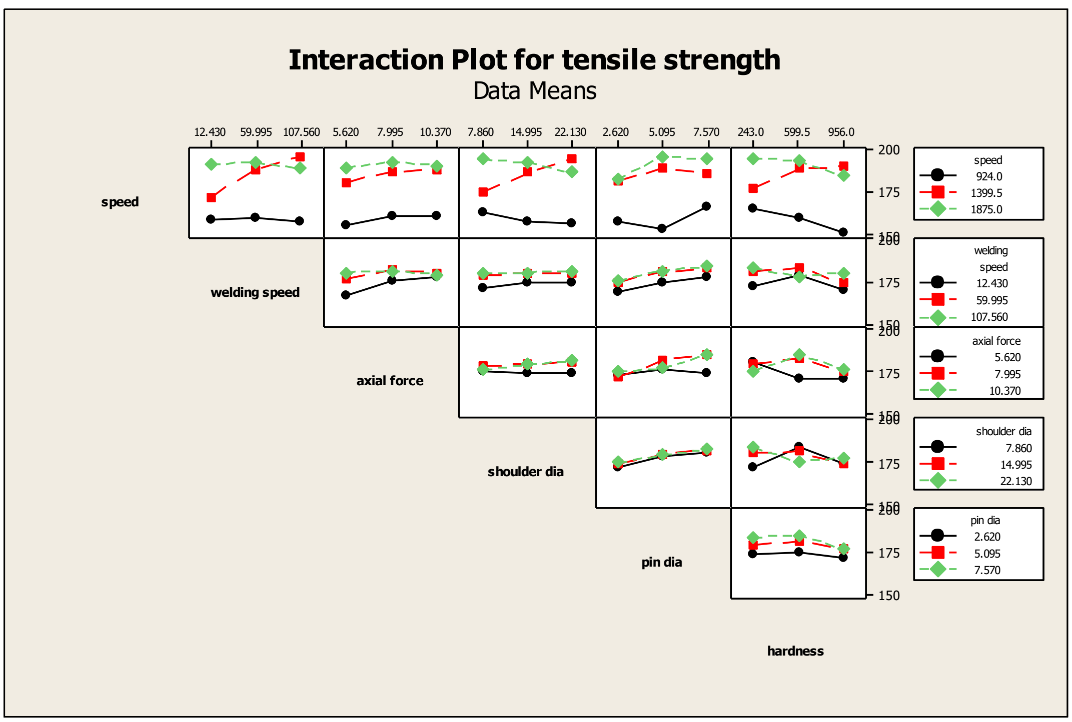

Fig.4.9. Interaction effect plots for tensile strength.

The main and interaction effects are plotted as shown in fig.4.8 and fig.4.9 of tensile strength. To analyse the main effects plots for tensile strength, the rotational speed is 924 rpm, welding speed is 12.430mm/min, the axial force is 5.62kN, shoulder diameter is 7.86mm, pin diameter 2.62mm and hardness are 956HV. These whole values didn't break the mean line so that got a better result with these combinations.

4.2.1. Regression Analysis.

The statistically significant mathematical model is achieved by using the regression analysis. The residual plots of regression analysis with the response of weld nugget grain size and tensile strength as shown in the fig.4.6 and fig.4.7. The residual plots contain normal probability plot, versus fits, histogram, and versus order graphs. All the graphs are fitted with the residue. The p-value is a measure of the strength of the evidence in the data against H_0(null hypothesis). Usually, the smaller the p-value, the stronger the sample evidence is for rejecting H_0. The least value of that causes H 0 to be rejected is the p-value, to be more precise. When the value of the p-test is more than 0.05, we do an ANOVA. ANOVA is a statistical method used to determine if the means of two or more groups differ from one another substantially. ANOVA compares the means of various samples to examine the influence of one or more factors.

The numerous actions The ANOVA family includes ANOVA. Because it compares the mean scores of two groups on various observations, the repeated measures ANOVA is comparable to the dependent sample T-Test. The cases in one observation must be closely related to the cases in all other observations for the repeated measures ANOVA to be valid. Using repeated observations as the basis, the repeated measures ANOVA compares means for one or more variables. The number of independent variables in a repeated measures ANOVA model can either be zero or more. Once more, at least one dependent variable in a repeated measures ANOVA has more than one observation.

5. CONCLUSIONS

In conclusion, the generation of a neural model to achieve perfect welds (negative welds) of FSW was performed on AA 6061-T6 aluminium alloy by combining six input parameters (speed rotation, welding speed, longitudinal force, shoulder diameter, glass pin and tool stiffness). Generate residual, principal effects, and interactive effects diagrams of friction stirrups. The developed relationships can be effectively used to predict grain size and tensile strength of AA6061-T6 friction welded aluminium alloy joints in the range.

6. ACKNOWLEDGEMENTS

We thank all the teaching staff and non-teaching staff members of department of mechanical engineering who have helped us directly or indirectly during the paper work and helping hands in mechanical laboratories in SNIT College of Engineering. I also thank my co-authors for their valuable affectionate guidance in the writing paper.

REFERENCE

[1] "*PART VII JOINING & ASSEMBLY PROCESSES FUNDAMENTALS OF WELDING*," [Online]. Available: https://www.egr.msu.edu/~pkwon/me477/welding.

[2] "*Solid State Welding*," [Online]. Available: http://www.totalmateria.com/Article51.htm.

[3] F. Zhi-hong, H. Di-qiu, and W. Hong, "Friction Stir Welding of Aluminum Alloys 1 Introduction Microstructure of FSW Influential Factors of Weld Quality," *J. Wuhan Univ. Technol. Sci. Ed., vol. 19, no. 1, 2004.*

[4] Abey Vishnu Narayana, N. Ajayakumar, and M. J. Jose, "*Tool Pin Profiles and the Quality of Welds in Friction Stir Welding of Aluminium Alloys*," *Int. Conf. Mater. Mech. Manag.*, p. 9, 2020.

[5] K. P. Yuvaraj, P. Ashoka Varthanan, and C. Rajendran, "*Effect of friction stir welding parameters on mechanical and micro structural behaviour of AA7075-T651 and AA6061 dissimilar alloy joint*," *Int. J. Comput. Mater. Sci. Surf. Eng., vol. 7, no. 2*, pp. 130–149,2018,doi:10.1504/IJCMSSE.2018.092553.

[6] R. S. Mishra and Z. Y. Ma, "*Friction stir*

welding and processing," *Mater. Sci. Eng. R Reports, vol. 50, no. 1–2, pp. 1–78, 2005, doi: 10.1016/j.mser.2005.07.001.*

[7] J. Shen, Y. Li, T. Zhang, D. Peng, D. Wang, and N. Xu, "*Preheating friction stir spot welding of Mg/Al alloys in various lap configurations,*" *Sci. Technol. Weld. Join., vol. 20, no. 1, pp. 1–10, 2015, doi: 10.1179/1362171814Y.0000000248.*

[8] M. Bilgin, Ş. Karabulut, and A. Özdemir, "*Study on the Mechanical Properties of Dissimilar Friction Stir Welding of AA 7075 T6 and AZ31B Alloys*," *Proc. 2018 9th Int. Conf. Mech. Aerosp. Eng. ICMAE 2018*, pp. 467471,2018,doi:10.1109/ICMAE.2018.8467679.

[9] T. Medhi, M. K. Yadava, B. S. Roy, and S. C. Saha, "*An experimental investigation on implications of traverse speed in joining of dissimilar Al–Cu by friction stir welding*," *Int. J. Adv. Manuf. Technol., vol. 104, no. 1–4,* pp. 1461–1471, 2019, doi: 10.1007/s00170-019-04086-2.

[10] S. Rajakumar, C. Muralidharan, and V. Balasubramanian, "*Influence of friction stir welding process and tool parameters on strength properties of AA7075-T6 aluminium alloy joints,*" *Mater. Des., vol. 32, no. 2*, pp. 535549,2011,doi:10.1016/j.matdes.2010.08.025.

[11] B. Meyghani, M. B. Awang, S. S. Emamian, M. K. B. Mohd Nor, and S. R. Pedapati, "*A comparison of different finite element methods in the thermal analysis of friction stir welding (FSW)*," *Metals (Basel)., vol. 7, no. 10*, pp. 1–23, 2017, doi: 10.3390/met7100450.

[12] S. V. and R. Raju, "*Process parameter optimization and characterization of friction stir welding of aluminum alloys*," *Int. J. Appl. Eng. Res., vol. Vol. 3, Is, no*. Gale Academic OneFile, Accessed 4 july, p. 1303+, [Online]. Available: https://go.gale.com/ps/anonymous?id=GALE%7CA216041272&sid=googleScholar&v=2.1&it=r&linkaccess=abs&issn=09734562&p=AONE&sw=w.

[13] P. M. G. P. Moreira, A. M. P. de Jesus, A. S. Ribeiro, and P. M. S. T. de Castro, "*Fatigue crack growth in friction stir welds of 6082-T6 and 6061-T6 aluminium alloys: A comparison*," *Theor. Appl. Fract. Mech.*, vol. 50, *no. 2*, pp. 81–91, 2008, doi: 10.1016/j.tafmec.2008.07.007.

[14] S. SHANAVAS and J. EDWIN RAJA DHAS, "*Parametric optimization of friction stir welding parameters of marine grade aluminium alloy using response surface methodology*," *Trans. Nonferrous Met. Soc. China (English Ed., vol. 27, no. 11*, pp. 2334–2344,2017,doi:10.1016/S10036326(17)60259-0.

[15] M. J. Peel, "*The friction-stir welding of dissimilar aluminium alloys*," 2005.

[16] N. Dialami, M. Cervera, and M. Chiumenti, "*Effect of the tool tilt angle on the heat generation and the material flow in friction stir welding," Metals (Basel)., vol. 9, no. 1*, 2019, doi: 10.3390/met9010028.

[17] H. Okuyucu, A. Kurt, and E. Arcaklioglu, "*Artificial neural network application to the friction stir welding of aluminum plates," Mater. Des., vol. 28, no. 1*, pp. 78–84, 2007, doi: 10.1016/j.matdes.2005.06.003.

[18] Frigaard, Grong, and O. T. Midling, "*A process model for friction stir welding of age hardening aluminum alloys*," *Metall. Mater. Trans. A Phys. Metall. Mater. Sci., vol. 32, no. 5,* pp. 1189–1200, 2001, doi: 10.1007/s11661-001-0128-4.

[19] H. W. Zhang, Z. Zhang, and J. T. Chen, "*3D modeling of material flow in friction stir welding under different process parameters," J. Mater. Process. Technol., vol. 183, no. 1,* pp.6270,2007,doi:10.1016/j.jmatprotec.2006.09.027.

[20] D. Fersini and A. Pirondi, "*Analysis and modelling of fatigue failure of friction stir welded aluminum alloy single-lap joints," Eng. Fract. Mech., vol. 75, no. 3–4*, pp. 790–803,2008,doi:10.1016/j.engfracmech.2007.04.013.

[21] G. Buffa, L. Fratini, and R. Shivpuri, "*CDRX modelling in friction stir welding of AA7075-T6 aluminum alloy: Analytical approaches," J. Mater. Process. Technol., vol. 191, no. 1–3*, pp.356359,2007,doi:10.1016/j.jmatprotec.2007.03.033.

[22] L. Fratini and G. Buffa, "*CDRX modelling in*

friction stir welding of aluminium alloys," Int. J. Mach. Tools Manuf., vol. 45, no. 10, pp. 1188-1194,2005,doi:10.1016/j.ijmachtools.2004.12.001.

[23] A. R. Shahani and A. Farrahi, "*Experimental investigation and numerical modeling of the fatigue crack growth in friction stir spot welding of lap-shear specimen," Int. J. Fatigue, vol. 125, no. April*, pp. 520–529, 2019, doi: 10.1016/j.ijfatigue.2019.04.026.

[24] A. Shahani and A. Farrahi, "*Effect of stirring time on the mechanical behavior of friction stir spot weld of Al 6061-T6 lap-shear configuration," Proc. Inst. Mech. Eng. Part C J. Mech. Eng. Sci., vol. 233, no. 10*, pp. 3583–3591, 2019, doi: 10.1177/0954406218818606.

[25] Firouz Fadaeifard, M. R. Pakmanesh, M. S. Esfahani, K. A. Matori, and D. Chicot, "*Nanoindentation Analysis of Friction Stir Welded 6061-T6 Al Alloy in As-Weld and Post Weld Heat Treatment," Phys. Met. Metallogr., vol. 120, no. 5*, pp. 483–491, 2019, doi: 10.1134/S0031918X1905003X.

[26] B. Wu, J. Liu, Q. Song, Z. Lv, and W. Bai, "*Controllability of joint integrity and mechanical properties of friction stir welded 6061-T6 aluminum and AZ31B magnesium alloys based on stationary shoulder," High Temp. Mater. Process., vol. 38, no. 2019*, pp. 557–566, 2019, doi: 10.1515/htmp-2019-0001.

[27] T. Singh, S. K. Tiwari, and D. K. Shukla, "*Effect of nano-sized particles on grain structure and mechanical behavior of friction stir welded Al-nanocomposites," Proc. Inst. Mech. Eng. Part L J. Mater. Des. Appl., vol. 234, no. 2*, pp. 274–290, 2020, doi: 10.1177/1464420719885156.

[28] J. Yoon, C. Kim, and S. Rhee, "*Compensation of vertical position error using a force–deflection model in friction stir spot welding," Metals (Basel)., vol. 8, no. 12*, 2018, doi: 10.3390/met8121049.

[29] A. R. Torabi, M. H. Kalantari, and M. R. M. Aliha, "*Fracture analysis of dissimilar Al-Al friction stir welded joints under tensile/shear loading," Fatigue Fract. Eng. Mater. Struct., vol. 41, no. 9*, pp. 2040–2053, 2018, doi: 10.1111/ffe.12841.

[30] Z. Liu, S. Ji, and X. Meng, "*Joining of magnesium and aluminum alloys via ultrasonic assisted friction stir welding at low temperature," Int. J. Adv. Manuf. Technol., vol. 97, no. 9–12*, pp. 4127–4136, 2018, doi: 10.1007/s00170-018-2255-8.

[31] M. Assidi and L. Fourment, "*Accurate 3D Friction Stir Welding simulation tool based on friction model calibration," Int. J. Mater. Form., vol. 2, no. SUPPL*. 1, pp. 327–330, 2009, doi: 10.1007/s12289-009-0541-6.

[32] F. Liu, L. Fu, and H. Chen, "*Microstructure Evolution and Mechanical Properties of High-Speed Friction Stir Welded Aluminum Alloy Thin Plate Joints," J. Mater. Eng. Perform., vol. 27, no. 7*, pp. 3590–3599, 2018, doi: 10.1007/s11665-018-3441-4.

[33] A. Niroumand-Jadidi and S. F. Kashani-Bozorg, "*Microstructure and property assessment of dissimilar joints of 6061-T6 Al/dual-phase steel fabricated by friction stir spot welding," Weld. World, vol. 62, no. 4*, pp. 751–765, 2018, doi: 10.1007/s40194-018-0602-x.

[34] F. J. Liu, L. Fu, and H. Y. Chen, "*Microstructure evolution and fracture behaviour of friction stir welded 6061-T6 thin plate joints under high rotational speed," Sci. Technol. Weld. Join., vol. 23, no. 4*, pp. 333–343,2018,doi:10.1080/13621718.2017.1389837.

[35] Y. Yue, Z. Zhang, S. Ji, Z. Li, and D. Yan, "*Friction stir lap welding of 6061-T6 Al to Ti-6Al-4V using low rotating speed," Int. J. Adv. Manuf. Technol., vol. 96, no. 5–8*, pp. 2285–2291, 2018, doi: 10.1007/s00170-018-1769-4.

[36] S. Rajakumar, C. Muralidharan, and V. Balasubramanian, "*Establishing empirical relationships to predict grain size and tensile strength of friction stir welded AA 6061-T6 aluminium alloy joints," Trans. Nonferrous Met. Soc. China (English Ed., vol. 20, no. 10*, pp. 1863–1872, 2010, doi: 10.1016/S1003-6326(09)60387-3.